
ORIGINAL ARTICLE

Early warning signals in plant disease outbreaks

S. Orozco-Fuentes¹ | G. Griffiths¹ | M. J. Holmes² |
R. Ettelaie² | J. Smith² | A. W. Baggaley¹ | N. G.
Parker¹

¹School of Mathematics, Statistics and
Physics, Newcastle University, Newcastle
upon Tyne, NE1 7RU, UK

²School of Food Science and Nutrition,
University of Leeds, Leeds, LS2 9JT, UK

Correspondence

Sirio Orozco-Fuentes

Email:

sirio.orozco-fuentes@newcastle.ac.uk

Summary

1. Infectious disease outbreaks in plants threaten ecosystems, agricultural crops and food trade. Currently, several fungal diseases are affecting forests worldwide, posing a major risk to tree species, habitats and consequently ecosystem decay. Prediction and control of disease spread are difficult, mainly due to the complexity of the interaction between individual components involved.

2. In this work, we introduce a lattice-based epidemic model coupled with a stochastic process that mimics, in a very simplified way, the interaction between the hosts and pathogen. We studied the disease spread by measuring the propagation velocity of the pathogen on the susceptible hosts. Quantitative results indicate the occurrence of a critical transition between two stable phases: local confinement and an extended epiphytotic outbreak that depends on the density of the susceptible individuals.

3. Quantitative predictions of epiphytotics are performed using the framework early-warning indicators for impending regime shifts, widely applied on dynamical systems. These signals forecast successfully the outcome of the critical shift between the two stable phases before the system enters the epiphytotic regime.

4. *Synthesis:* Our study demonstrates that early-warning indicators could be useful for the prediction of forest disease epidemics through mathematical and computational models suited to more specific pathogen-host-environmental interactions.

KEYWORDS

Plant-pathogen interactions, Lattice model, Tree disease,
Early-warning signals, Disease triangle, Plant-plant interactions,
Plant pathology

1 | INTRODUCTION

Invasive non-indigenous pathogens and vectors such as fungi, bacteria and insects pose a serious threat to trees and forest health worldwide. The recent and well-publicised outbreak of the ash dieback fungus (*Hymenoscyphus pseudoalbidus*) and emerald ash borer (*Agilus planipennis*) risks the survival of the ash tree (*Fraxinus excelsior*) in the UK (Mitchell et al., 2014; Thomas, 2016), one of the most abundant trees in small woodlands and high forests across the country (National Forestry Inventory, 2014). At the same time, it threatens its extinction across the European continent (Gross et al., 2014).

Historically, these events cause catastrophic ecological, economic and social impact, and motivate a detailed understanding of the mechanisms that underlie the epidemics, from which strategies to manage and prevent future occurrences can be developed systematically (Mitchell et al., 2014). The propagation of these infectious agents to the susceptible population depends on a plethora of biological, geographical, climatic and anthropological factors. For example, epidemics mediated by vectors influence the spread of the pests, particularly over long range distances, through accidental dispersal and international plant trade and transportation (Macnadbay et al., 2004; Alfinito et al., 2016). The mobility and viability of the pathogens vary with weather and the seasons, and on larger time-scales the increasing temperatures due to climate change are believed to promote the survival and dispersal of invasive pests (Bebber et al., 2013; Parepa et al., 2013).

Forests reunite all the features and characteristics of a complex adaptive system, in which multiple components interact non-linearly and in such intricate ways over long temporal scales (Messier et al., 2013; Filotas et al., 2014). Due to their age and size distributions, trees have different degrees of susceptibility to pathogens and period of infectiousness (Gross et al., 2014). In addition, intermingling trees of different species play a crucial role in the spread of pathogens despite having immunity. For example, some trees can serve as *reservoirs* of inoculae and aid in the disease transmission to the highly susceptible taxa (Xu et al., 2009; Prospero and Cleary, 2017). Even though, trees are sessile, their spatial distribution is highly clustered following irregular patterns. Forest pathogens reshape the landscape of woodlands and forests, which, in turn, affect future outbreaks (Condeso and Meentemeyer, 2007). These factors make the behaviour of the system as a whole, difficult to predict under perturbations such as disease outbreaks.

Mathematical modelling provides a powerful approach to understand, predict and counter-act disease propagation. Early-warning indicators for abrupt changes in the behaviour of complex systems, group a set of statistical properties measured on parameters that change in unique ways before the occurrence of a catastrophic shift, (also known in the literature as tipping point or critical transition), which occurs when a system switches abruptly between alternate equilibria (Scheffer et al., 2009; Scheffer, 2009). These indicators are generic and suitable for application across many system types, even if the underlying system dynamics are poorly understood (Carpenter and Brock, 2006; Scheffer et al., 2009; Morales et al., 2015).

In ecosystems, early-warning methods have been used to predict the occurrence of desertification processes (Corrado et al., 2014), animal extinction in deteriorating environments (Drake and Griffen, 2010), behaviour of aquatic ecosystems (Gsell et al., 2016), and have been applied on climate models for the simulation of dieback on the Amazon rainforest (Boulton et al., 2013). Therefore, their usefulness to predict changes on degradation processes for biological systems has increased in the literature during the last decade (Carpenter and Brock, 2006; Scheffer et al., 2009; Dakos et al., 2012; Litzow and Hunsicker, 2016; Gsell et al., 2016; Ratajczak et al., 2017). The main purpose behind these indicators is their effectiveness to identify properties in an ecological system that would change significantly as it approaches a tipping point between different stable states. However, this idea has been applied only to a handful of ecological problems due to the unavailability of data sets, (Gsell et al., 2016; Litzow and Hunsicker, 2016; Ratajczak et al., 2017).

Our interest lies in analysing the dynamics of disease outbreaks under the scope of classical early-warning techniques. This suggests applying the universality class and scaling exponents—which have been widely studied in the literature (Bunde and Havlin, 1996; Stauffer and Aharony, 2003)—to the prediction and detection of the transition from the progression of the disease to an epiphytotic outbreak.

The structure of the paper is as follows. In §2, we propose a simplified model of a forest, in terms of susceptible, infected or removed individuals (SIR model) which exhibits a phase transition above a percolation threshold (Grassberger, 1993; Clar et al., 1996; Bunde and Havlin, 1996). In §3, we show the results of the simulations in which, we quantify the propagation velocity of the infection. Then, we obtain the phase diagram of the contained-to-outbreak phases of the system and study the behaviour of relevant parameters. Finally, in §4 we discuss the meaning and implications of our findings.

2 | MATERIALS AND METHODS

We model a forest as a regular square lattice of dimensions $L \times L$ where $L = 500$, see Fig. 1. The forest landscape is flat and there is only one type of vegetation. Each site can exist in one of four states: susceptible (S), infected (I), removed (R) and empty (\emptyset). Susceptible individuals correspond to a population of healthy trees distributed randomly which can become infected. An infected node, represents a patch of vegetation that has acquired a terminal disease, a removed node corresponds to the space left by the infected node after the vegetation dies, and empty nodes correspond to sites in the landscape where no susceptible vegetation can grow. The location of the forest patches is constant in time, such that vegetation nodes (either S , I or R) are randomly distributed with a density ρ .

Once a node in the S category acquires an infection, its status is changed to I and a numerical label η is attached to it. η increases with time at a constant pace, ranging from $-T$ to 0. Whereupon at $\eta = 0$, the population at the site dies and the node is removed, i.e., its status is changed to R . Henceforth, T corresponds to the infectious period, that is, the time in which any infected tree can transmit the infection.

After a tree is infected, it has a probability β of transmitting the disease to a neighbouring susceptible site during the infectious period. In epidemiological terms, the probability β is denoted as the transmissibility of the pathogen, and it is defined as the probability per unit time that an S node acquires the infection from a neighbouring I node. For simplicity, the neighbourhood is defined by the first four nearest neighbours in the lattice, i.e., a von Neumann neighbourhood.

We consider the limit in which the disease spreads in a much smaller time-scale than the growth of the susceptible species. Moreover, after a patch of forest has died, there exists the possibility of invasion from another species of plant, a phenomenon which has been observed in grass-woodland transitions (Abades et al., 2014). As a consequence, it is unlikely that the woodland site regains susceptibility, and thus, we neglect any regenerative process in the simulations.

The parameters β and T regulate the evolution of the disease and both are relevant in the model; sampling from a suitable distribution for each parameter would allow to model levels of disease tolerance to the pathogen for each tree, since it has been identified that some plants exhibit little damage despite a high level presence of the pathogen (Gross et al., 2014).

For simplicity, in our simulations, we consider uniform values for β and T . This implies that we are free to set the time-scale by fixing a value for either variable. The time evolution of the landscape is carried out in discrete unitary time intervals. Therefore, by setting $T = 10$, a unitary time interval corresponds to $0.1T$. This leaves the average vegetation density, ρ , and the transmissibility of the pathogen, β , as two free parameters.

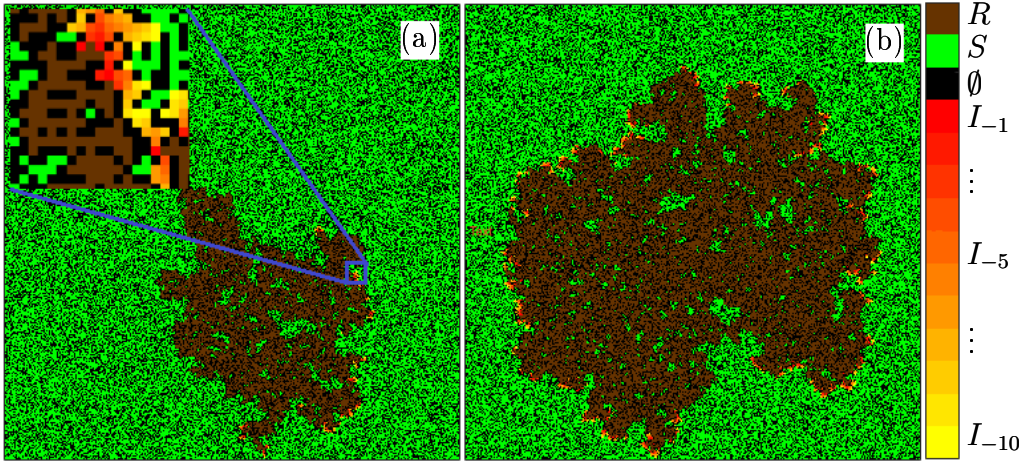


FIGURE 1 Final configurations of disease spread obtained for a system with $L = 500$, $\beta = 0.5$ and tree densities $\rho = 0.60$ (a) and 0.62 (b). Near the critical transition, slight changes in tree densities result in different spatial patterns of disease spread. *Inset*: Detail of the nodes statuses with trees represented following the colourbar showed on the right: empty (\emptyset), susceptible (S), removed (R) and infected (I).

3 | RESULTS

At the beginning of the simulation, the disease is introduced as a clump of infected trees at the centre of the domain as a square shape of size $\ell = L/100$. This was found to be sufficient in order to avoid extinction of the disease at initial stages. Under these conditions the transient time, i.e., the time lapse that contains remnants of the initial conditions, was found to be ~ 200 time steps. Since we are interested in the steady regime, we discarded this transient from our final calculations. The simulations run until the infected nodes disappear or, in order to avoid boundary effects, when infected nodes reach any of the four sides. We carried out simulations over 10^4 ensemble realisations.

As a first step, we quantify the effect of ρ and β in the simulations. At low ρ , the infection quickly dies out, since the distribution of hosts is sparse. On the other side, for higher densities, the epidemic spreads out, infecting most of the trees. Nonetheless, for certain densities, the system shows a critical transition between a self-limited outbreak and a large-scale epiphytotic outbreak.

In Fig. 1, we show the final configuration ($t \sim 600$ time-steps) of the landscape for densities below and above the critical transition. Near the critical transition, the pathogen spreads through the domain generating branching structures, and patches of surviving trees may remain unaffected. To highlight this result, in Fig. 2, we show the spatio-temporal behaviour of the number of infected hosts averaged over the width of the domain for densities $\rho = 0.58$ (a), $\rho = 0.60$ (b) $\rho = 0.62$ (c) and $\rho = 0.80$ (d), following the same parameters as in Fig. 1. We find that a transition in the severity of the disease occurs in the interval $[0.56, 0.64]$.

At the critical transition, the disease does not annihilate all the tree population, but rather spreads through the lattice as active clusters of diseased trees, interspersed with healthy individuals.

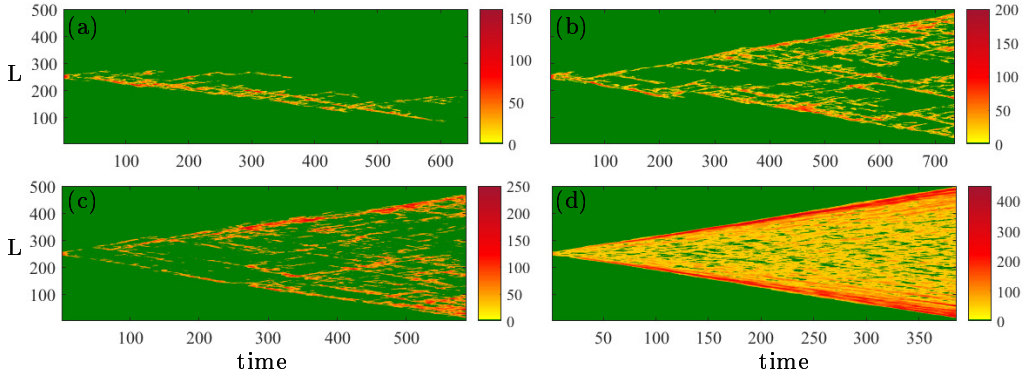


FIGURE 2 Spatio-temporal behaviour of the number of infected hosts averaged over the width of the domain for varying tree densities ρ : (a) 0.58, (b) 0.60, (c) 0.62 and (d) 0.80. The colour bar shows the number of infected trees per averaged line. The first three cases (a-c) correspond to values in the critical region $\rho \approx \rho_c$ and although the disease is spreading through the domain is not annihilating all susceptible hosts, since there are green patches interspersed with diseased trees.

3.1 | The Phase Diagram

The spreading of the disease has the effect of separating two domains, healthy susceptible trees, S , and dead trees, R by a transient interface of infected individuals, I . In this model, the number of affected nodes is on average, proportional to the landscape area where the infection has been present. By construction, this constant of proportionality is $1/\rho$, and thus, the proportion of affected woodland is

$$A = \frac{N}{\rho}, \quad (1)$$

where N is the sum of the I and R nodes.

To quantify the observed dynamics in this system we calculated the spread dynamics of the disease through the lattice via the effective¹ velocity v of the pathogen. On this basis of Eq. 1, a characteristic length-scale, $\mathcal{R} = N^{1/2}$, measures of the radial extent of the disease. Thus, the rate of propagation of the disease in the domain is measured through the velocity v , defined as the change in \mathcal{R} , i.e.,

$$v(t) = N^{1/2}(t) - N^{1/2}(t-1). \quad (2)$$

Therefore, Eq. 2 measures the spreading velocity in terms of the area of sick trees in the domain. The time series of v is shown in Fig. 3(a-c); we will show that the stochasticity observed in these time series gives valuable information about the underlying dynamics when analysed in the framework of early warning indicators for critical transitions.

¹We use the term "effective" to emphasize that strictly the velocity cannot be defined in this way close to the critical density since the spanning cluster of diseased trees becomes fractal. It can be rigorously shown that the velocity with which the disease front propagates is given in 2D as $v \sim \xi^{1-d_f/d_\ell} \sim (\rho - \rho_c)^{0.16}$, with ξ denoting the correlation length, d_f and d_ℓ the fractal and graph dimensions respectively, (Bunde and Havlin, 1996). However, Eq. 2 provides a convenient measure of the rate of spread of the infection, through the epidemic extent or area, which is usually monitored through observational data, (Cowger et al., 2005; Mundt et al., 2013).

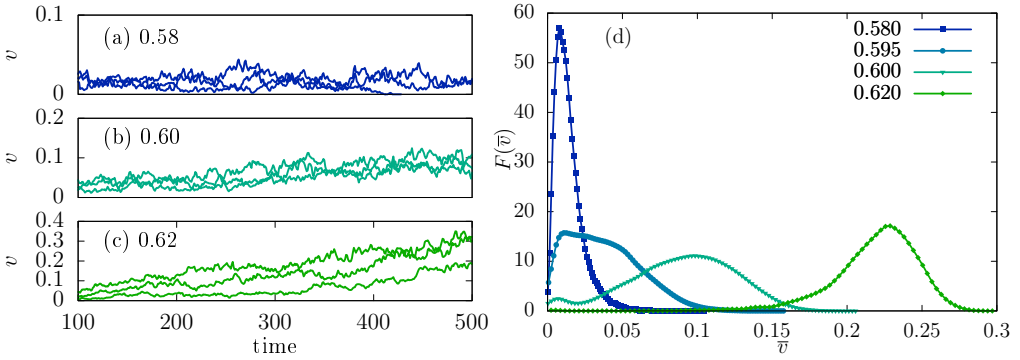


FIGURE 3 (a-c) Time series for the propagation velocity $v(t)$ for the following values of tree densities: (a) $\rho = 0.58$, (b) $\rho = 0.60$ and (c) $\rho = 0.62$. Three samples are showed for each density. (d) Probability distribution function $F(\bar{v})$ for the time averaged velocity \bar{v} obtained from 10^4 simulations, for densities $\rho = [0.58, 0.595, 0.6, 0.62]$. For all cases $L = 500$ and $\beta = 0.5$.

From the time series for the velocity, we obtain the time average of the velocity \bar{v} . Figure 3(d) shows several probability distribution functions $F(\bar{v})$ obtained from all realisations, for the following densities $\rho = 0.58, 0.595, 0.6$ and 0.62 . For $\rho < \rho_c$, the distribution shows a maximum for $\bar{v} \sim 0.01$, see curve for $\rho = 0.58$. As the tree density increases, and approaches the critical value, $\rho = 0.595$ and $\rho = 0.6$, $F(\bar{v})$ shows clearly that the system can be found in either two states, one for $\bar{v} \approx 0$, which corresponds to local disease confinement and another for $\bar{v} \neq 0$, or epiphytotic outbreak. As the density increases, e.g., $\rho = 0.62$, the probability distribution function shows a single maximum for $\bar{v} = 0.24$.

After taking the ensemble averages we obtain the mean propagation velocity $\langle \bar{v} \rangle$ as a function of the tree density ρ and various values of the transmission probability β . We identify from these results a critical density that separates the non-spreading to spreading phase of the disease. The existence of a critical density at ρ_c implies the existence of a spatially connected or spanning cluster of trees for disease spread. From these results, we conclude that this critical density ρ_c , is similar in nature to the critical percolation threshold observed in percolation theory (Stauffer and Aharony, 2003; Gandolfi, 2013; Saberi, 2015), since our computational model only involves a slight modification of the former.

In Fig. 4, we observe that the sole effect of the transmission probability $\beta = [0.1, 1]$ is a displacement of the critical point towards lower values of ρ . For low disease transmissibility, the density of trees has to be high to have a spanning cluster through the domain. As β increases, there is a chance of infecting more trees per infectious period (T) and consequently this cluster occurs at lower densities. Therefore, T , acting conjointly with β define the limiting value ρ_c . As β is increased, the critical transition should tend to the percolation threshold reported in the literature, $\rho_c \rightarrow 0.592746$ (Stauffer and Aharony, 2003). However, since we are working on a finite-size domain, we expect that the critical transition is broadened relative to the result above for infinite-sized domains; in Fig. 4(a) we highlight this as a shaded region that divides density values according to a region where the critical shift occurs in our simulations (the black dotted line highlights the result for $\beta = 0.5$).

3.2 | Catastrophic shifts in forest disease

A fundamental emergent property observed in systems near criticality is their capacity to extend over scales comparable to the size of the whole system at long times. Near the critical threshold, short-range interactions lead to the emergence of long-range correlations and the behaviour of the system changes abruptly between two alternative stable states, in

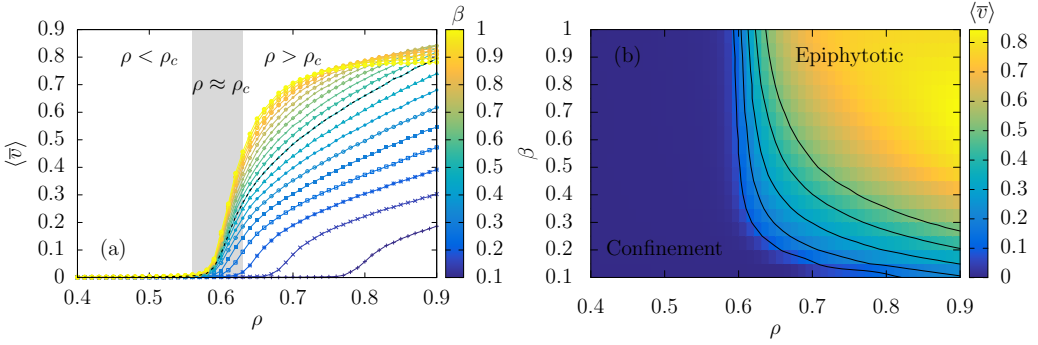


FIGURE 4 (a) Propagation velocity $\langle \bar{v} \rangle$ for the spread of a pathogen inside a grid with dimensions $L = 500$ as a function of tree density ρ and disease transmissibility β , following a Von Neumann neighbourhood. A shift between two stable states: infection confinement and an extended epiphytotic outbreak, occurs for $\rho \approx \rho_c$. A shaded region is showed for $\rho \sim \rho_c$, associated with the black dotted line highlighting the results for $\beta = 0.5$. (b) Phase space diagram for the pathogen dispersal on the grid, indicating region of disease containment and epiphytotics.

this case, local containment and epiphytotics. The occurrence of this shift depends only on the local structure (density) of susceptible hosts. Near the critical transition this system exhibits scale invariance, self-similarity and fractal properties. From the non-stationarity of the time series showed in Fig. 3(a-c) we can analyse the underlying dynamics through metric-based indicators proposed in the literature for the identification of early-warning signals: variance, skewness, kurtosis and autocorrelation function at lag 1 (Carpenter and Brock, 2006; Dakos et al., 2012; Morales et al., 2015).

Our goal is to predict the occurrence of a transition between disease containment and epiphytotics using the theory of catastrophic shifts, which in principle could be useful for the prediction of patterns of disease spread in forests.

We quantify the stochastic variability of $v(t)$ from time series obtained for an ensemble of systems evolving for fixed $\beta = 0.5$ on a domain of size $L = 500$. Our interest was to study the variability in the spread velocity as the density of trees crosses the critical region. From the probability distribution functions for $\langle \bar{v} \rangle$, we obtained the ensemble behaviour of the following statistical measures: variance (a), kurtosis (b), skewness (c) and autocorrelation function at lag 1 (d), see Fig. 5. All results were obtained using MATLAB (2016).

The variance, in Fig. 5(a), shows a rise around the critical point, the increase of this quantity is maximal, and its behaviour is different before the transition occurs, for $\rho < \rho_c$ and after it has happened, $\rho > \rho_c$. The square-root of the variance, the standard deviation, is maximal at the critical transition, which for this finite-size system is $\rho^{\max} = 0.61$. Therefore, this quantity is useful as an indicator for the prediction of a shift between the disease confinement and epidemics.

The skewness, defined as the third moment of the distribution, quantifies the asymmetry of fluctuations in the time series. It is a useful measure for the prediction of the catastrophic shift since its value changes before and after the transition, depending on whether the system settles down to an alternative state in which the disease propagation is larger or smaller than in the current state, (Guttal and Jayaprakash, 2008; Dakos et al., 2012; Kéfi et al., 2014). Our results clearly show both an increase and further decrease in the skewness, see Fig. 5(b). For $\rho < \rho_c$ the skewness is positive and rises up as we approach the critical region. For $\rho \sim \rho_c$, it decreases abruptly and changes sign, becoming negative, i. e., the probability distribution is left-skewed. As we increase the density of trees and drive the system away from the critical region, the skewness changes again, and becomes less negative until it settles near zero (≈ -0.5). Notably, the rise in skewness observed at $\rho \sim 0.57$, associated with an increase in the nonlinearities of the time series, predicts the outcome of the tipping point. Moreover, this parameter identifies the tree densities for which the system is

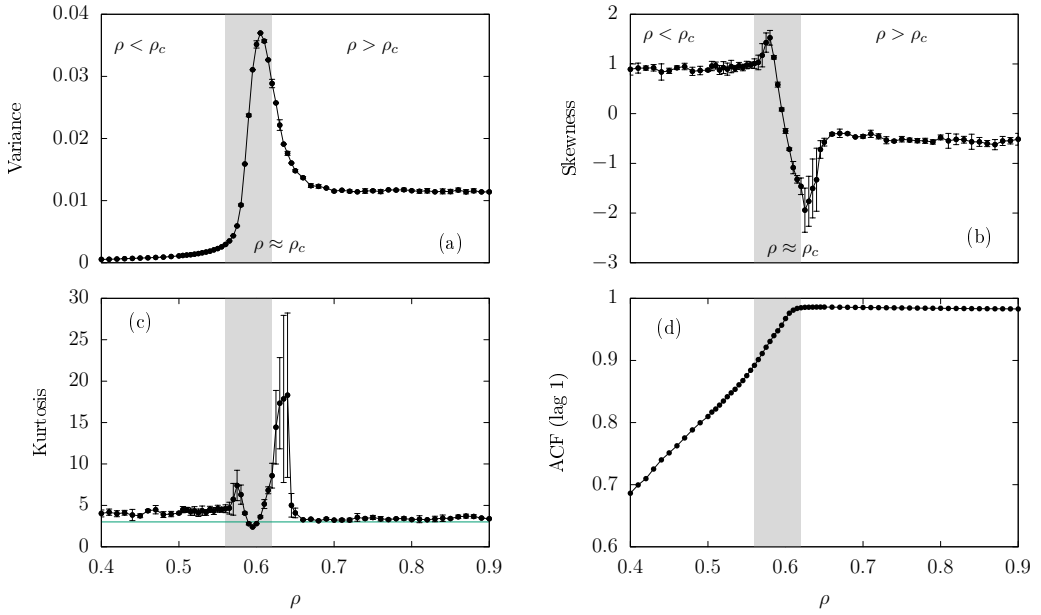


FIGURE 5 Ensemble behaviour for the metric-based indicators measured for the propagation velocity v of disease spread in the domain ($L = 500$, $\beta = 0.5$). Temporal variance (a), kurtosis (b), skewness (c) and autocorrelation function at lag $\tau = 1$, as a function of the tree density ρ . Three regimes are shown, with the shaded area corresponding to $\rho \approx \rho_c$.

found in either disease confinement (Skewness ≈ 1) and epiphytotic (Skewness ≈ 0).

Strong perturbations can drive the state of a system to reach extreme values close to a transition. Therefore, the probability distribution function of the propagation velocity may show a rise in the kurtosis before the transition is reached. Figure 5(c) shows the plot of this quantity obtained in our simulations. The distribution shows two peaks: a local maximum that corresponds to kurtosis values of 7.4 for $\rho \approx 0.57$, and a global maximum with kurtosis of 18.3 for $\rho \approx 0.64$. This indicates that, as the system approaches and exits the critical region, the distribution becomes more strongly peaked, than the reference normal distribution, which has a kurtosis of 3 (blue continuous line), and thus, is leptokurtic. This is consistent with an increased presence of rare values in the propagation velocity. Interestingly, for values closer to the critical point, i. e., $\rho = 0.59$, the kurtosis is 2.4, which is equivalent to a flattened or platykurtic distribution. We conclude that the kurtosis is a good indicator to detect the outcome of the transition.

The temporal autocorrelation function (ACF) measures the spectral properties and changes in the correlation structure, “memory”, of the time series (Dakos et al., 2012). In a general way, the τ^{th} order ACF is defined accordingly as,

$$ACF(\tau) = \frac{\sum_{t=\tau+1}^n (v_t - \bar{v})(v_{t-\tau} - \bar{v})}{\sum_{t=1}^n (v_t - \bar{v})^2}. \quad (3)$$

Following equation 3, we measured the temporal autocorrelation function at lag 1 ($\tau = 1$) in our simulations. Several dynamical systems have shown a slow recovery from small perturbations as they approach the critical transition, phenomenon termed in the literature as “critical slowing down”. These systems show an increase in the short-term memory of time series which can be detected through an increase of the autocorrelation function at lag 1.

Figure 5(d) show the values for the temporal autocorrelation function at lag 1 measured for the time series of the velocity as a function of the tree density ρ . For $\rho < \rho_c$, this quantity increases linearly as we increase the tree density and reaches a maximum threshold inside the critical region for $\rho \geq 0.6$. This is an indication that the system has become increasingly similar between consecutive observations. Since, for $\rho < \rho_c$ there is a fast increase on the ACF, this is useful for the prediction of the outcome of the critical shift in the system.

4 | DISCUSSION

The most important question during risk assessment for a forest disease is how pathogens will spread on the landscape, both to predict the occurrence of an epiphytotic outbreak and to assist in designing interventions to counter the onset and progression of the disease. In a real life scenario, the dispersal of these diseases is complex, mainly due to the multiple geographical and environmental factors affecting the disease spread.

Lattice-based epidemic models have been used previously in the literature to study temporal and spatial fluctuations on the prevalence of epidemic diseases in terms of the minimum population density for an epidemic to occur (Rhodes and Anderson, 1996, 1997). The sessility of trees makes lattice modelling of plant diseases more attainable through computational simulations. Works on disease propagation using this framework coupled with historical, geographical and weather information have been used previously to predict the spread of pathogens through forests (Xu et al., 2009; Meentemeyer et al., 2010; Potter et al., 2011; Cobb et al., 2012). These models certainly capture some of the features of previous epiphytotics, and coupling them to the framework of early-warning indicators for detecting critical transitions could be useful for designing strategies against disease spread.

The following characteristics needs to be fulfilled for an epidemic to occur: (i) a critical number of susceptible hosts, (ii) an aggressive phenotype of the pathogen with a high transmissibility rate and (iii) suitable environmental conditions for the pathogen survival. In this paper, we chose to study the effect of the two first factors using a generic stochastic model of epidemic spread on a lattice with a von Neumann neighbourhood. Our model does not incorporate a sophisticated computational description of the system; however it is useful, as a first approximation, for the application of the framework of early warning signals, used widely on complex systems, to reach a new understanding in plant disease epidemics.

Simulations for different tree densities and pathogen transmission indicate a system that shows two stable states: disease confinement and an extended epiphytotic outbreak. We chose to focus our investigations on densities that may result in the system be found in either state. All the indicators measured forecast the occurrence of the critical transition. We observe a rise in the variance, skewness and the autocorrelation function at lag 1 as the system approaches $\rho \sim \rho_c$. The skewness also shows a steep change from a positive to a negative value in this region, consistent with the system traversing the critical region and reaching a new stable state. Similarly, the kurtosis, changes from leptokurtic to platykurtic and leptokurtic again in the critical region and immediately afterwards. Consequently, we conclude that all these measures are applicable to predict a transition to epiphytotics.

Although our current scenario of applicability is a regular domain, far away from the heterogeneous and complex landscapes found in real forests which involves large scales, we hypothesize that their applicability to plant diseases could be fruitful in predicting the outcome of major disease outbreaks. In real datasets, one of the first challenges would be to define a set of parameters and coarse-grain the system description to an appropriate scale (spatial resolution of the ecological data) to apply these indicators to predict a range of future states of disease propagation.

Currently, remote sensing technologies, such as satellites and aerial photography are used widely to obtain forest measurements on droughts, fire damage and extent of disease propagation. Since this information is periodically

updated, these datasets can be transformed into spatial patterns and time series of epidemic extent which could be used to detect the approach to a tipping point before it is crossed.

Particularly, the UK has an advantageous position on GIS forest datasets such as the National Forestry Inventory (NFI) (Forest-Research, 2016), Light Detection And Ranging (LiDAR) (Forest-Research, 2004) and the National Tree Map® (NTM)(Bluesky-International-Limited, 2017), which give accurate information about the woodland patches, 3D forest structure and location and canopy extent of individual trees over 3 m in height, respectively. Moreover, the currently running SAPPHIRE project (Forest-Research, 2018), a collaboration between Forest Research and Rezatec will provide precision maps of tree species and pinpoint trees that exhibit features of stress and disease. Combining all these together, the applicability of early-warning indicators on a complex adaptive system, such as forests, could prove fruitful for devising their stability and resilience to external conditions (such as disease propagation) before a regime shift occurs.

ACKNOWLEDGEMENTS

We thank Dr Willem Roelofs and Dr Alan Macleod for discussions, and financial support from Defra. S. A. Orozco-Fuentes would like to thank to E. R. Gutierrez and A. P. Riascos for comments on early versions of the manuscript.

DATA ACCESSIBILITY

This papers does not use data.

AUTHOR CONTRIBUTIONS

SOF, NGP and AWB conceived the ideas and designed methodology; SOF implemented the computational model and led the writing of the manuscript. SOF and GG analysed the data. NGP, AWB, MJH, JS and RE acquired the funding. All authors contributed critically to the drafts and gave final approval for publication. The authors declare no conflicts of interest.

REFERENCES

- Abades, S. R., Gaxiola, A. and Marquet, P. A. (2014) Fire, percolation thresholds and the savanna forest transition: a neutral model approach. *Journal of Ecology*, **102**, 1386 – 1393.
- Alfinito, E., Beccaria, M. and Macorini, G. (2016) Critical behaviour in a stochastic model of vector mediated epidemics. *Scientific Reports*, **6**.
- Bebber, D. P., Ramotowski, M. A. T. and Gurr, S. J. (2013) Crop pests and pathogens move polewards in a warming world. *Nature Climate Change*, **3**, 985–988.
- Bluesky-International-Limited (2017) National Tree Map. URL: <https://www.blueskymapshop.com/products/national-tree-map>.
- Boulton, C. A., Good, P. and Lenton, T. M. (2013) Early warning signals of simulated Amazon rainforest dieback. *Theoretical Ecology*, **6**, 373–384. URL: <https://doi.org/10.1007/s12080-013-0191-7>.
- Bunde, A. and Havlin, S. (1996) *Fractals and Disordered Systems*. Springer.
- Carpenter, S. R. and Brock, W. A. (2006) Rising variance: a leading indicator of ecological transition. *Ecology Letters*, **9**.

- Clar, S., Drossel, B. and Schwabl, F. (1996) Forest fires and other examples of self-organized criticality. *Journal of Physics: Condensed Matter*, **8**, 6803 – 6824.
- Cobb, R. C., Filipe, J. A. N., Meentemeyer, R. K., Gilligan, C. A. and Rizzo, D. M. (2012) Ecosystem transformation by emerging infectious disease: loss of large tanoak from california forests. *Journal of Ecology*, 712–722.
- Condeso, T. E. and Meentemeyer, R. K. (2007) Effects of landscape heterogeneity on the emerging forest disease sudden oak death. *Journal of Ecology*, **95**, 364–375.
- Corrado, R., Cherubini, A. M. and Pennetta, C. (2014) Early warning signals of desertification transitions in semiarid ecosystems. *Physical Review E*, **90**, 062705.
- Cowger, C., Wallace, L. D. and Mundt, C. C. (2005) Velocity of spread of wheat stripe rust epidemics. *Ecology and Epidemiology*, **95**, 972–982.
- Dakos, V., Carpenter, S. R., Brock, W. A., Ellison, A. M., Guttal, V., Ives, A. R., Kéfi, S., Livina, V., Seekell, D. A., van Nes, E. H. and Scheffer, M. (2012) Methods for detecting early warnings of critical transitions in time series illustrated using simulated ecological data. *PLOS ONE*, **7**, 1–20. URL: <https://doi.org/10.1371/journal.pone.0041010>.
- Drake, J. M. and Griffen, B. D. (2010) Early warning signals of extinction in deteriorating environments. *Nature*, **467**, 456–459.
- Filotas, E., Parrott, L., Burton, P. J., Chazdon, R. L., Coates, K. D., Coll, L., Haeussler, S., Martin, K., Nocentini, S., Puettmann, K. J., Putz, F. E., Simard, S. W. and Messier, C. (2014) Viewing forests through the lens of complex systems science. *Ecosphere*, **5**, 1 – 23.
- Forest-Research (2004) Light Detection and Ranging (lidar). URL: <https://www.forestry.gov.uk/fr/lidar>.
- (2016) National Forest Inventory. URL: <https://www.forestry.gov.uk/inventory>.
- (2018) Space Applications for Precision Plant Health Information, Response and Evaluation (sapphire). URL: <https://www.forestry.gov.uk/fr/sapphire>.
- Gandolfi, A. (2013) Percolation methods for SEIR epidemics on graphs. In *Dynamic Models of Infectious Diseases* (eds. S. H. R. V. and D. R.), chap. 2. Springer.
- Grassberger, P. (1993) On a self-organized critical forest-fire model. *Journal of Physics A: Mathematical and General*, **26**, 2081.
- Gross, A., Holdenrieder, O., Pautasso, M., Queloz, V. and Sieber, T. N. (2014) Hymenoscyphus pseudoalbidus, the causal agent of european ash dieback. *Molecular Plant Pathology*, **15**, 5–21.
- Gsell, A. S., Scharfenberger, U., Özkundakci, D., Walters, A., Hansson, L.-A., Janssen, A. B. G., Nöges, P., Reid, P. C., Schindler, D. E., Van Donk, E., Dakos, V. and Adrian, R. (2016) Evaluating early-warning indicators of critical transitions in natural aquatic ecosystems. *Proceedings of the National Academy of Sciences*, **113**, E8089–E8095.
- Guttal, V. and Jayaprakash, C. (2008) Changing skewness: an early warning signal of regime shifts in ecosystems. *Ecology Letters*, **11**, 450–460.
- Kéfi, S., Guttal, V., Brock, W. A., Carpenter, S. R., Ellison, A. M., Livina, V. N., Seekell, D. A., Scheffer, M., van Nes, E. H. and Dakos, V. (2014) Early warning signals of ecological transitions: Methods for spatial patterns. *PLOS ONE*, **9**, 1–13.
- Litzow, M. A. and Hunsicker, M. E. (2016) Early warning signals, nonlinearity, and signs of hysteresis in real ecosystems. *Ecosphere*, **7**.
- Macnadbay, E., Bezerra, R., Fulco, U., Lyra, M. and Argolo, C. (2004) Critical behavior of a vector-mediated propagation of an epidemic process. *Physica A: Statistical Mechanics and its Applications*, **342**, 249 – 255.
- MATLAB (2016) *version 9.0.0 (R2016a)*. Natick, Massachusetts: The MathWorks Inc.

- Meentemeyer, R. K., Cunniffe, N. J., Cook, A. R., Filipe, J. A. N., Hunter, R. D., Rizzo, D. M. and Gilligan, C. A. (2010) Epidemiological modeling of invasion in heterogeneous landscapes: spread of sudden oak death in california (1990-2030). *Ecosphere*, **2**, 1–24.
- Messier, C., Puettmann, K. J. and Coates, K. D. (2013) *Managing Forests as Complex Adaptive Systems*. Editorial Routledge.
- Mitchell, R., Beaton, J., Bellamy, P., Broome, A., Chetcuti, J., Eaton, S., Ellis, C., Gimona, A., Harmer, R., Hester, A., Hewison, R., Hodgetts, N., Iason, G., Kerr, G., Littlewood, N., Newey, S., Potts, J., Pozsgai, G., Ray, D., Sim, D., Stockan, J., Taylor, A. and Woodward, S. (2014) Ash dieback in the uk: A review of the ecological and conservation implications and potential management options. *Biological Conservation*, **175**, 95 – 109.
- Morales, I. O., Landa, E., Angeles, C. C., Toledo, J. C., Rivera, A. L., Temis, J. M. and Frank, A. (2015) Behavior of early warnings near the critical temperature in the two-dimensional ising model. *PLOS ONE*, **10**, 1–20.
- Mundt, C. C., Wallace, L. D., Allen, T. W., Hollier, C. A., Kemerait, R. C. and Sikora, E. J. (2013) Initial epidemic area is strongly associated with the yearly extent of soybean rust spread in north america. *Biol. Invasions*, **15**, 1431–1438.
- Parepa, M., Fischer, M. and Bossdorf, O. (2013) Environmental variability promotes plant invasion. *Nature Communications*, **4**.
- Potter, C., Harwood, T., Knight, J. and Tomlinson, I. (2011) Learning from history, predicting the future: the uk dutch elm disease outbreak in relation to contemporary tree disease threats. *Philosophical Transactions of the Royal Society B*, **366**, 1966–1974.
- Prospero, S. and Cleary, M. (2017) Effects of host variability on the Spread of Invasive Forest Diseases. *Forests*, **8**, 1–21.
- Ratajczak, Z., D'Odorico, P., Nippert, J. B., Collins, S. L., Brunsell, N. A. and Ravi, S. (2017) Changes in spatial variance during a grassland to shrubland state transition. *Journal of Ecology*, **105**, 750 – 760.
- Rhodes, C. and Anderson, R. (1997) Epidemic thresholds and vaccination in a lattice model of disease spread. *Theoretical Population Biology*, **52**, 101–118.
- Rhodes, C. J. and Anderson, R. M. (1996) Dynamics in a lattice epidemic model. *Physics Letters A*, **210**, 183–188.
- Saberi, A. A. (2015) Recent advances in percolation theory and its applications. *Physics Reports*, **578**, 1–32.
- Scheffer, M. (2009) *Critical Transitions in Nature and Society*. Princeton University Press.
- Scheffer, M., Bascompte, J., Brock, W. A., Brovkin, V., Carpenter, S. R., Dakos, V., Held, H., van Nes, E. H., Rietkerk, M. and Sugihara, G. (2009) Early-warning signals for critical transitions. *Nature*, **461**.
- Stauffer, D. and Aharony, A. (2003) *Introduction to Percolation Theory*. Taylor & Francis, revised edn.
- Thomas, P. A. (2016) Biological flora of the British Isles: *Fraxinus excelsior*. *Journal of Ecology*, **104**, 1158–1209.
- Xu, X., Harwood, T. D., Pautasso, M. and Jeger, M. J. (2009) Spatio-temporal analysis of an invasive plant pathogen (*phytophthora ramorum*) in England and Wales. *Ecography*, **32**, 504 – 516.